

Draft: To be submitted to *The Astrophysical Journal*

On the Incidence of Strong Gravitational Lensing by Clusters in the Las Campanas Distant Cluster Survey

Dennis Zaritsky

*Steward Observatory, University of Arizona, 933 North Cherry Avenue, Tucson, AZ 85721,
USA*

and

Anthony H. Gonzalez

*Department of Astronomy, University of Florida, 211 Space Sciences Bldg., Gainesville, Fl,
32611-2055, USA*

ABSTRACT

The observed incidence of strongly lensing clusters exceeds the predictions of a Λ CDM model by about a factor of 10. We revisit the observational side of this discrepancy by measuring the incidence of strong lensing in a subsample of clusters drawn from the Las Campanas Distant Cluster Survey (LCDCS). Among clusters with $0.5 \leq z \leq 0.7$, the redshift range in which we focus our search, we find two strongly lensed systems within an effective search area of 69 sq. deg. There is at least one other strongly lensed systems in the LCDCS outside of this redshift range, where we are less complete. Over all redshifts, the Λ CDM model produces one large arc every 146 sq. degrees. Assuming Poisson statistics, the probability of finding 3 or more strongly lensing clusters in 69 sq. degrees is 0.012. The lensing incidence within the LCDCS is in agreement with that derived from an X-ray selected sample and what has been preliminarily presented from an independent optical cluster survey. The origin of the disagreement between theory and observations, which remains at least at the order of magnitude scale for the Λ CDM model, lies either in the concordance cosmological model, in the characteristics of the resulting cluster potentials, or in the adopted source population.

1. Introduction

The “cosmic concordance” cosmological model, $\Omega_m = 0.3$, $\Omega_\Lambda = 0.7$, has quickly become the standard as a result of new observations (Type I supernovae by Riess et al. (1998) and Perlmutter et al. (1999); cosmic microwave background anisotropies by de Bernardis et al. (2000), Hanany et al. (2000), and Pryke et al. (2002)) and its ability to reconcile long-standing problems (for examples see Ostriker & Steinhardt (1995)). The only prominent partial holdout in this avalanche of evidence had been the distribution of QSO lens image separations (see Falco et al. (1998)), but even that discrepancy is now thought to be resolved (Keeton 2001). One less well known, but perhaps more striking discrepancy lies with the incidence of giant gravitational arcs in galaxy clusters. Bartelmann et al. (1998) found that the the currently favored Λ CDM underpredicts the strong lensing incidence among a sample of X-ray selected clusters by an order of magnitude. Because this discrepancy is one of the few pieces of observational evidence against what has become the accepted cosmological model, it warrants further examination on both the theoretical and observational fronts. We measure the incidence of lensing among clusters drawn from the Las Campanas Distant Cluster Survey (Gonzalez et al. 2001) and compare it to other measurements and to the existing theoretical expectations.

The potential use of the galaxy cluster mass function to probe the characteristics and evolution of the largest gravitationally bound structures, and therefore constrain the cosmological model, has been theoretically demonstrated over the past decade (see for examples Frenk et al. (1990), Eke, Cole, & Frenk (1996), and Evrard et al. (2002)). Unfortunately, there are various reasons why the study of clusters has yet to provide a wholly satisfying constraint. One of the most evident weaknesses had been the lack of large numbers of known clusters at higher ($z > 0.5$) redshifts. This weakness is being addressed with the many-fold growth in the number of known high redshift, massive clusters due in large part to a variety of both published (Postman et al. (1996), Scodreggio et al. (1999), Gonzalez et al. (2001)) and ongoing (Gladders and Yee (2000), Willick et al. (2001)) ground-based, optical surveys.

A second more pernicious difficulty involves the measurement of the cluster mass. The measurement is fraught with possible systematic errors and is observationally time-intensive. There are four ways to confirm that a cluster is massive: 1) compute the velocity dispersion using a large number (> 30) of member galaxy redshifts (for high- z clusters this requires several hours of observation per spectroscopic mask on 10m-class telescopes; see Lubin et al. (2002)), 2) measure the temperature of the intergalactic medium using X-ray observations (this requires exposures of tens of ksec per cluster on X-ray satellite telescopes; see Jeltama et al. (2001)), 3) construct a Sunyaev-Zel’dovich decrement map (this requires ~ 40 hours of on-source integration; see Joy et al. (2001)) or 4) measure the distortion of background

galaxy images introduced by the cluster’s gravitational potential (weak lensing maps require several hours of imaging on 10-m class telescopes; see Clowe et al. (2000)). The demanding observational requirements explain why there are relatively few high- z clusters with measured masses and create a significant impediment to taking full advantage of the hundreds of potential massive high- z clusters presented in the new catalogs.

A special case of method (4) is what is of interest here. Strong lensing, where the cluster potential distorts the image of a background image sufficiently that it appears as an arc (Lynds & Petrosian (1986), Soucail et al (1987)), is a rare phenomenon that increases in likelihood, in part, as the cluster mass increases (Luppino et al. (1999), Dahle et al. (2002)). The observational advantages of using strong lensing include that a relatively modest investment of telescope time per cluster is necessary, that it highlights the clusters with the greatest relaxed mass, and that it is a relatively unambiguous phenomenon at a properly selected magnitude limit. Theoretical studies (Bartelmann et al. (1998), Meneghetti et al. (2000), Meneghetti et al. (2001)) have found that the predicted numbers of strongly lensing clusters vary by orders of magnitude among popular cosmological models. The principal disadvantage of the strong lensing approach is that only a small fraction of clusters will produce gravitational arcs, so that even the results from large samples of clusters may suffer from small number statistics. Nevertheless, the differences among various models are sufficiently large that certain models can be excluded by a small number of lensing clusters. In particular, Bartelmann et al. (1998) found that Λ CDM models produce an order of magnitude too few giant arcs to match the observations available at that time.

We describe a study that is analogous to that conducted by Luppino et al. (1999), except that our sample is drawn from an optical survey and concentrates on a more limited redshift range ($0.5 \leq z \leq 0.7$). The cluster samples are entirely independent. The typical concerns regarding the viability and fidelity of optical cluster catalogs (contamination and projection effects) are less relevant here than in a measurement of the cluster mass function because any observed strong lensing confirms the cluster. As long as one realizes that this study provides a lower-limit on the lensing incidence, we avoid the concerns regarding optical cluster catalogs. In §2 we describe our sample and the observations. In §3 we present our newly discovered lensing clusters, calculate the incidence of lensing at these redshifts, compare that incidence to that found in other studies based on independent X-ray and optical catalogs, and compare our results to theoretical predictions. We summarize our findings in §4.

2. The Data

2.1. Sample Selection

The target clusters are a subsample of the Las Campanas Distant Cluster Survey (LCDCS; Gonzalez et al. (2001)). The catalog resulting from that survey contains 1073 candidate clusters at estimated redshifts, $z_{est} > 0.35$ in a statistically complete sample. For each candidate we provide the coordinates, an estimated redshift, which is based on the luminosity of the brightest cluster galaxy (BCG), and a central surface brightness measurement, Σ , which correlates broadly with standard mass estimators such as the X-ray temperature and luminosity, and velocity dispersion. Extensive testing, in the original catalog paper (Gonzalez et al. 2001), in work using our survey data to examine the evolution of the cluster galaxies and the BCG (Nelson et al. (2001a) and Nelson et al. (2001b)), and in the preliminary stages (Gonzalez et al. 2002) of the ESO Distant Cluster Survey (EDisCS) all confirm the contamination rates ($\sim 30\%$) and redshift uncertainties ($\Delta z < 0.1$ for $> 80\%$ of the candidates) derived in the survey paper.

Clusters in the LCDCS are detected as regions of excess surface brightness relative to the extragalactic background, by first removing all resolved stars and galaxies from the survey images and then convolving the data with a $10''$ exponential smoothing kernel (Gonzalez et al. 2001). Positive surface brightness fluctuations are induced by light from fainter, undetected cluster galaxies and extended emission from the halo of the brightest cluster galaxy. The peak amplitude of the detected surface brightness, Σ , effectively measures the integrated cluster light within a fixed, exponentially weighted aperture after removal of the brightest galaxies in the cluster. The value of Σ corrected for Galactic extinction is Σ_{cor} . Because of the shallow nature of the exposures (exposure times ~ 190 sec on a 1m telescope), only a few (< 10) cluster galaxies are typically detected and removed before smoothing (including any resolved interlopers). Σ is tied to the total cluster luminosity, with the caveats that more galaxies will be removed prior to smoothing in nearer systems, that the BCG may contribute significantly, and that the concentration of the cluster will affect Σ . These distance-dependent effects must be empirically calibrated and that calibration is currently somewhat uncertain due to the small number of X-ray clusters at $z > 0.7$ that we have been able to observe with the same instrumental configuration. For more details on this calibration we refer the reader to Gonzalez et al. (2001).

Using Σ_{cor} , we select the clusters that are likely to be the most massive systems in the catalog at $z_{est} \geq 0.5$. Because of the possible exclusion of massive clusters due to the scatter between Σ_{cor} and mass, the measured incidence of lensing from this sample, if quantified as the number of lenses per unit volume (or per steradian), will be a lower limit on the

true incidence. The two other potential problems with the LCDCS selection, the possible presence of “false” clusters in the sample due to contamination and the possible inclusion of less massive clusters because of scatter in Σ_{cor} –mass relation, will make our search less efficient but will not bias the lensing incidence if we express the quantity in terms of lenses per steradian. However, potential unknown biases, for example if the success of our method in identifying a cluster depends on a cluster property that also affects the likelihood of cluster lensing, such as the concentration of the mass profile, then some possible choices for the measure of the lensing incidence, such as the *fraction* of lensing clusters would be artificially inflated, while others, such as the number of lenses per steradian would be unchanged. Care must be taken in defining a quantification of incidence that is consistently a lower limit. We shall quote lensing incidence as a function of area of sky.

From the LCDCS catalog, we select candidate clusters with $0.5 \leq z_{est} \leq 0.85$ and $\Sigma_{cor} > 9.03 \times 10^{-3}$ cts s⁻¹ sq. arcsec⁻¹, which corresponds to a velocity dispersion, σ , greater than 390 km s⁻¹ at $z = 0.5$, 765 km s⁻¹ at $z = 0.7$, and 1040 km s⁻¹ at $z = 0.8$ (Gonzalez et al. 2001). These criteria produce a list of 125 candidates that we then classify visually. Some high surface brightness candidates are obvious low surface brightness galaxies or tidally interacting pairs and can be rejected immediately (of the 125 candidates, only six were identified to be such from the original survey data). Of the remaining 119 candidates, we select 66 as being the most promising, with the highest priority for observation. Independently selected, there is a sample of 30 LCDCS candidates that are being observed as part of the ESO Distant Cluster Survey, or EDisCS (19 of which fall within our selection criteria). We did not re-observe the 16 of these that fall within our high-priority list, nor the three that fall within our low-priority list.

2.2. Observations

We were able to observe 44 candidate clusters (40 from the high priority list and four from the low priority list) with the Baade 6.5m telescope on Las Campanas using the Magellan Instant Camera (MagIC) during 9 - 12 Mar 2002. The camera’s detector is a SiTe 2K by 2K device with a pixel scale of 0.069 arcsec pixel⁻¹ (field-of-view is 2.36’). We observed in the SDSS r' filter (Smith et al. 2002), with complementary g' observations for four clusters that showed interesting features in the initial r' frames. The exposure times are either 1800 or 2400 sec total, split between 3 frames (the total exposure times for each cluster are given in Table 1). The seeing was excellent for the four night observing run. The effective seeing (after registering the images and combining) is typically 0.5 to 0.6 arcsec, and is given for each cluster in Table 1.

The data reduction is only slightly more complicated than usual because the camera uses a four amplifier read-out mode to reduce the readout time. Therefore, bias and flatfielding is done differently for each quadrant. We applied the standard, public MagIC reduction pipeline to do the first order corrections and corrected for cosmic rays using the COSMICRAYS task in IRAF¹. We then use the Source Extractor (SExtractor) algorithm (Bertin & Arnouts 1996) to produce a background sky image (objects removed). We remove the spatially-variable background by subtracting this image from the original image. Images are then registered and combined using IMALIGN and IMCOMBINE tasks in IRAF. We run SExtractor on the final combined images to produce a catalog of objects in each target field and objects with stellarity index < 0.9 are considered to be galaxies. Our detection parameters are set conservatively to require a minimum of 10 pixels, each above a 1σ deviation above the global sky, for an object detection. We interactively define polygon apertures in the r' band to measure the magnitudes and colors of the lensed galaxies. Photometric calibration was done using both the SDSS calibration (Smith et al. 2002) and Landolt (1992) standards to place the photometry on both systems.

2.3. Sample Properties

The redshift and surface brightness, Σ_{cor} , distributions of the entire sample of 125 candidates and the subsample of observed clusters (including the EDisCS clusters) are shown in Figure 1. The only qualitative difference between the low and high priority clusters is that the high priority clusters are slightly more weighted toward lower redshifts. This difference is the result of lower-redshift candidates appearing more secure in the original survey data, and hence assigned a higher priority. The EDisCS observations will help fill in the high redshift tail of the range, while most of the clusters observed here lie between $0.5 < z_{est} < 0.7$. The right panels of the Figure illustrate the difficulty in defining a mass-limited sample. The steep rise in the number of clusters toward smaller masses means that a small systematic error could easily change the sample size by a factor of two and that random errors will generate significant contamination of the sample by lower-mass clusters.

The final desired quantity, the incidence of giant arcs, can be made independent of the uncertainty in the mass measurement by being sufficiently conservative in the mass cut used to define the imaging subsample. Because only high-mass clusters produce strong arcs (see Luppino et al. (1999)), a sufficiently low mass cut will ensure that all strongly-lensing

¹IRAF is the Image Reduction and Analysis Facility written by the NOAO, which is operated by AURA under cooperative agreement with the National Science Foundation.

clusters are in the subsample. The disadvantage of such an approach is that the number of clusters to observe is correspondingly larger. The advantage of a catalog with more precise mass measurements, such as X-ray luminosity or temperature, is primarily in the efficiency with which one can initially identify the candidate lensing clusters, but all studies should find the lensing clusters.

To examine the effects of our adopted mass cut, we plot Σ_{cor} vs. z_{est} for our sample and two curves that illustrate where our calibration of the $L_X - \Sigma_{cor}$ relationship places the two L_X limits from previous studies² in Figure 2. The lower curve corresponds to $L_X = 4.7 \times 10^{44} h_{50}^{-2}$ ergs s⁻¹, the limit below which previous studies found no strongly lensing clusters (Luppino et al. 1999). The upper curve corresponds to $L_X = 1.2 \times 10^{45} h_{50}^{-2}$ ergs s⁻¹, a cluster luminosity at which previous studies found that over 50% of clusters act as strong lenses (Luppino et al. (1999), Dahle et al. (2002)). Our sample would include all of the most-likely LCDCS lensing clusters ($L_X > 1.2 \times 10^{45} h_{50}^{-2}$ ergs s⁻¹) for $0.5 \leq z \leq 0.7$, *if there was no scatter in our $L_X - \Sigma_{cor}$ calibration*. We include clusters below the $L_X = 4.7 \times 10^{44} h_{50}^{-2}$ ergs s⁻¹ line at low z because our estimation of L_X using Σ_{cor} has roughly a factor of two scatter (Gonzalez et al. 2001). At $z \sim 0.7$ the scatter in the relationship implies that we are potentially missing some strongly-lensing clusters in our survey. An important aspect of the calibration that is yet not well-measured is the redshift evolution. In making the Figure we adopt a $(1+z)^4$ evolution in the optical surface brightness, even though a fit to limited data available suggests a steeper slope (Gonzalez 2000). Adopting the latter behavior would make the curves decline more steeply than shown in the Figure and would suggest that we are even less complete in our sample of high-mass clusters at high-redshift than illustrated in Figure 2. We are currently unable to be sufficiently conservative in our inclusion of all possible lensing clusters at these redshifts because of the limited number of candidates that we can follow-up. As such, this adds another reason why we consider our result to be a lower limit on the incidence of lensing at these redshifts.

2.4. Arcs

We visually examine each of the cluster images. To match previous work we are attempting primarily to identify arcs that extend at least $\sim 10''$ and have $R < 21.5$. These criteria place these images well above our detection thresholds. In the last column of Table

²We convert all luminosities from the literature for an $\Omega_m = 1$ cosmology to the open cosmology ($\Omega_m = 0.3, \Omega_\Lambda = 0$) used by Gonzalez (2000) in determining the various relationships used here. For this reason, the numerical values are generally ~ 1.2 times the published values.

1, we present comments regarding the candidate cluster (‘marginal’ reflects the status of the cluster candidate, not of any potential arc-like feature). We identify three clusters that exhibit features that appear to be gravitationally lensed galaxies (LCDCS 280, 486, and 954, see Figure 3-5). For these three clusters we also identify several additional (sometimes questionable) features that may be lensed images. However, we do not identify similar low-quality features in other cluster fields because of their uncertainty as lensed images. A summary of their magnitudes and colors is presented in Table 2. The magnitudes of the “lensed” images ranges from 20.07 to 24.25 in r' , while the faintest detected objects in the frame are typically at least two magnitudes fainter. The galaxy count histograms typically peak at a magnitude of between 23 and 24, and only thereafter exhibit serious incompleteness. No cluster has a histogram that peaks brighter than $r' = 22$, which is 2 magnitudes fainter than our criteria for identifying the principal lensed image in a cluster.

2.4.1. LCDCS 280

This is the least convincing case of lensing among the three clusters in which we have found “lens-like” images. Both lens features 1 and 2 consist of four peaks, each around a different apparent mass center in the cluster. The luminous galaxy near lens feature 1 is a typical, extended brightest cluster galaxy. Lens features 3,4,5, and 6 are all quite marginal cases of lensing, but they appear curved with a center of curvature near the BCG. Spectroscopy of lensed features 1 and 2 is possible with a large telescope (sources are brighter than $R = 22$ and the irregular structure may be indicative of emission line regions).

Assuming that the images are lensed, we estimate the mass producing the lensing by adopting the singular isothermal sphere (SIS) potential, measuring the distance from the lensed image to the center of curvature (R_L), and making an assumption that the source distance is twice that of the lens. As such, the velocity dispersion of the SIS potential is given by $\sigma_{300} = \sqrt{(R_L/1.3'')}$. Defining the center of curvature is somewhat ambiguous in these cases, but we explore two possibilities: 1) we visually fit a circle through the suspected lensed images ($R_L = 7.5''$), and 2) we take the center to be coincident on the nearby dominant galaxy ($R_L = 3.6''$). In the former case, we calculate that $\sigma = 720 \text{ km s}^{-1}$, and in the latter that $\sigma = 500 \text{ km s}^{-1}$. The latter case suggests that if these are lensed images, we may be seeing group/galaxy lensing rather than cluster lensing. The former is a plausible cluster lens velocity dispersion, but is significantly larger than the dispersion calculated from Σ_{cor} , 520 km s^{-1} , using the relationship between Σ_{cor} and σ from Gonzalez et al. (2001).

Given the various difficulties in convincingly identifying these images as lensed images and our intent to maintain our measurement as a lower limit, *we will not count this object*

as a lensing cluster. Further observations are necessary to confirm the lensed nature of these images.

2.4.2. LCDCS 486

This cluster contains the brightest of the arc features found in this study (and the brightest of any of the arcs listed in the Luppino et al. (1999) compendium; their Table 2). We measure that the arc has a length, l , of $13.7''$ a length-to-width ratio, l/w , of 10.9 (12.5 if the width has the effect of seeing removed by simple quadrature), and an average surface brightness of $R = 22.9$ mag sq. arcsec. The one potentially suspicious aspect of this arc is the sharp bend in the middle. A possible interpretation is that we are seeing a superposition of an arc (or two) and an unlensed galaxy. However, the $g' - r'$ color is highly uniform along the entire length (the color of the entire arc matches that of the primarily horizontal portion, 1a, and that of the primarily vertical portion, 1b, to 0.02 mag). The rather unusual arc morphology implies a challenge to the modeling of this system, but the length, the degree of curvature, and uniform colors suggest that this is indeed a lensed image.

Applying the same simple mass model as above (for a measured $R_L = 9''$, we estimate the velocity dispersion of the corresponding SIS model to be 790 km s^{-1} . From Σ_{cor} we estimate that $\sigma = 750 \text{ km s}^{-1}$. The agreement between the two σ estimates further supports the lensing interpretation of this image.

2.4.3. LCDCS 954

This is the most “classic” lens of the three systems, with some other lensed features also visible in the image. In particular, lens feature 2 is a potential radial arc. The principal arc has $l = 9.4''$, $l/w = 9.0$ (11.7 when the width is corrected for the effect of seeing), and an average surface brightness of $R = 23.8$ mag/sq. arcsec. This is the most massive (as measured by Σ_{cor} corrected for redshift) cluster in our sample for $0.5 \leq z < 0.7$ and shows the most dramatic lensing. Such überclusters are exceedingly rare. Given the effective area of the LCDCS (69 sq. deg; (Gonzalez et al. 2001)) and the discovery of one such system at these redshifts, we expect only about 600 similar clusters in the Universe at $0.5 < z < 0.7$. There is a similar known cluster RX J1347.5–1145 in the LCDCS (LCDCS 829) at slightly lower redshifts, 0.45, (which also produces gravitational arcs; Sahu et al. (1998)) and has a measured bolometric L_X somewhere between $9 \times 10^{45} h_{50}^{-2}$ and $2.4 \times 10^{46} h_{50}^{-2} \text{ ergs s}^{-1}$; Schindler et al. (1997), Ettori et al. (2001)). For a local comparison, the Coma cluster has

$L_X = 2.4 \times 10^{45} h_{50}^{-2}$ ergs s^{-1} (Ebeling et al. 1998). For a distant comparison, MS1054.4–0321, which is the best-studied X-ray luminous massive cluster at $z \sim 0.8$ has $L_X = 5.7 \times 10^{45} h_{50}^{-2}$ (Jeltema et al. 2001), with a well-measured weak lensing signal (Hoekstra et al. 2000) but no strong lensing. LCDCS 829 is known to be more X-ray luminous than these two well-known clusters, and LCDCS 954 is expected to be more luminous based on its value of Σ_{cor} .

Again, we estimate the mass of the system by fitting an SIS model for a measured $R_L = 21.8''$. We calculate that $\sigma = 1230$ km s^{-1} . The estimated σ derived from Σ_{cor} is 1670 km s^{-1} . There is some discrepancy in these estimates, but both suggest that this is a very massive cluster.

3. Discussion

Although we have repeatedly noted that this study will provide a lower limit on the lensing incidence, a measurement that is far below the true incidence may provide little constraint on cosmological models. There are two primary reasons why our measurement could be a gross underrepresentation of the true value. First, the LCDCS could be severely incomplete in the most massive clusters. Second, even if the LCDCS is complete, our subsample could be incomplete if our conversion between Σ_{cor} and mass is faulty. We argue against both of these possibilities below and then present a comparison of our measurement of the lensing incidence to observational and theoretical studies.

3.1. Number Density of Massive Clusters

To determine whether the LCDCS is missing a significant fraction of potential lensing clusters, we compare the number densities of massive clusters in the LCDCS and in the *Einstein Medium Sensitivity Survey* (EMSS). We restrict our analysis to $0.4 < z < 0.6$, where the $T_X - \Sigma_{cor}$ relation is best determined (and does not involve the highly uncertain redshift correction), and to $L_X > 10^{45} h_{50}^{-2}$ ergs s^{-1} cm^{-2} , where the EMSS catalog is less incomplete.

Within the effective area of the primary, statistical LCDCS catalog (69 sq. degrees), we detect 9 cluster candidates at $0.4 < z \leq 0.6$ with surface brightnesses that imply $L_X > 10^{45} h_{50}^{-2}$ ergs s^{-1} . This result yields a raw angular density of $(13 \pm 4 \pm 4) \times 10^{-2}$ clusters per square degree (to minimize dependence on cosmological models we calculate and compare angular densities). The first quoted uncertainty reflects Poisson counting; the second reflects the systematic uncertainty from the conversion of Σ_{cor} to L_X (a $1-\sigma$ variation in this relation results in a net change in sample size of ± 4 clusters). There are several further steps in

converting this raw density to a true density.

Because the number of clusters rises rapidly as mass decreases, significant scatter in Σ_{cor} or L_X , which is certainly present in the LCDCS, will artificially boost the number of clusters found above an imposed mass or L_X threshold. Redshift uncertainty and contamination in the LCDCS catalog also act to amplify the observed number of clusters. To assess the effect of scatter in the L_X conversion on the number density, we approximate the underlying cluster mass function with a Press-Schechter distribution (Press & Schechter 1974). This distribution is then multiplied by a transfer function to reproduce the effect of imposing a fixed mass limit. For data with a Gaussian uncertainty in mass, this yields

$$\frac{d\tilde{N}(M)}{dM} = \frac{dN(M)}{dM} \frac{1 - \text{erf}((M - M_{lim})/\sqrt{2}\sigma_M)}{1 + \text{erf}(M/\sqrt{2}\sigma_M)}, \quad (1)$$

where $d\tilde{N}/dM$ is the number of clusters of a given mass that are included in the sample, dN/dM is the initial Press-Schechter mass function, σ_M is the uncertainty in M , and M_{lim} is the mass limit of the survey imposed by the observer. To connect virial mass to L_X , we use the $L_X - T_X$ relation of Xue & Wu (2000) in conjunction with the equation

$$M_{vir} = 10^{15} \left(\frac{1.15\beta T_X}{1+z} \right)^{3/2} [\Omega_0 \Delta_{vir}(z)]^{-1/2} h_{50}^{-1} M_\odot, \quad (2)$$

which relates virial mass to X-ray temperature for a spherically symmetric, isothermal plasma in virial equilibrium (cf. Eke, Cole, & Frenk (1996) and Borgani et al. (1998)). The quantity $\Delta_{vir}(z)$ is defined as in Kitayama & Suto (1996), and we set $\beta=1$. For the LCDCS, the uncertainty is consistent with arising primarily from observational uncertainty (i.e. σ_Σ is constant), so $\sigma_M/M \approx 3.45 \times \sigma_\Sigma/\Sigma \approx 0.42(L_X/10^{45})^{-0.14}$ for $\sigma_\Sigma = 1.85 \times 10^{-3}$ counts s^{-1} arcsec^{-2} (see Gonzalez et al. (2001) for the origin of this value). The EMSS has the same qualitative problem, but the uncertainty in L_X is dominated by intrinsic scatter (i.e. the fractional uncertainty Σ_{L_X}/L_X is roughly constant), so $\sigma_M/M \approx 0.5 \times \sigma_{L_X}/L_X \approx 0.23$ for $\sigma_{\log L_X}=0.2$. For an imposed threshold of $L_X = 10^{45} h_{50}^{-2}$ ergs s^{-1} cm^{-2} there will be $\sim 21\%$ more clusters included in the LCDCS sample than in the EMSS sample due to the larger scatter in optically estimated mass.

Redshift uncertainties lead to a similar bias in which the more numerous, poorer clusters at $z < 0.4$ are scattered into the relevant redshift range. Although poorer, the surface brightnesses of these systems can be comparable to the more massive clusters at $z > 0.4$ because of the redshift dependence of Σ . We again use the PS formalism to compute the expected number of clusters above the LCDCS detection threshold as a function of redshift, and then convolve this distribution with the redshift uncertainty (see Gonzalez et al. 2001 for the

functional form of the redshift uncertainty). The redshift bias introduces an additional 19% increase in the observed surface density.

Finally, contamination of the LCDCS sample by sources such as low surface brightness galaxies also boosts the observed surface density. For the redshift range $0.4 < z < 0.6$, we expect, on the basis of spectroscopy and imaging, that $\sim 80\%$ of the sources are real clusters (Zaritsky *et al.* 1997; Gonzalez *et al.* 2001; Nelson *et al.* 2001a). Accounting for all of the issues described above yields a corrected LCDCS surface density of $(7.2 \pm 2.4 \pm 2.4) \times 10^{-2}$ clusters per square degree with $L_X > 10^{45} h_{50}^{-2}$ ergs s^{-1} .

The EMSS contains five systems with bolometric luminosity $L_X > 10^{45} h_{50}^{-2}$ ergs s^{-1} cm^{-2} in this redshift range. Following the method of Henry *et al.* (1992) and Luppino & Gioia (1995), we compute the number density of EMSS clusters and obtain a comoving density of $9.6 \times 10^{-8} h^3$ Mpc^{-3} for $\Omega=1$, $\Lambda = 0$, which corresponds to a projected density of $(1.6 \pm 0.7) \times 10^{-2}$ clusters per square degree, where the quoted error is purely Poissonian. This value is 4.5 times smaller than the LCDCS value.

Why such a large discrepancy? Massive clusters are strongly correlated (see Gonzalez *et al.* (2002) for an analysis of the LCDCS) and the LCDCS sample includes RX J1347.5, which is the most luminous known X-ray cluster. Several other massive clusters are in close proximity to RX J1347.5, and consequently, the inadvertent inclusion of this particularly rich region of space in the LCDCS positively biases our computed angular density. To estimate the magnitude by which this correlation may impact the results, we recompute the angular density using only clusters that are at least 30 arcmin away from RX J1347.5 ($\sim 100 h^{-1}$ Mpc at $z=0.5$). With this restriction we have only 4 clusters in the remaining 60 square degrees (i.e. 56% of the most massive clusters in the LCDCS at $0.4 \leq z < 0.6$ are located within a region corresponding to 15% of the total survey area). Including correction for the statistical biases cited above yields a revised angular density of $(3.7 \pm 1.8_{-0.9}^{+1.8}) \times 10^{-2}$ clusters per square degree for the LCDCS. This value is 50% lower than that derived for the entire survey and not significantly ($< 2\sigma$) discrepant with the EMSS value. We conclude that the two surveys are marginally consistent with one another but that even in surveys that span over 100 sq. degrees it is possible to be significantly (factor of two) affected by large scale clustering. In particular, given that the number density from the LCDCS is larger than that from the EMSS, we conclude that the LCDCS is not missing a large number of potential lensing clusters out to at least $z = 0.6$.

3.2. Testing the Σ_{cor} –Mass Correlation

The degree to which we have identified all of the possible lensing clusters within the LCDCS for our follow-up imaging depends on the validity of the Σ_{cor} –mass relationship and its scatter. The empirical relation between the surface brightness of the original low surface brightness detection image and the mass of a cluster is only broadly established (Gonzalez et al. 2001). We will continue to test and refine this relationship because with a large survey it is necessary to develop a method to estimate cluster masses, even crudely, from the original survey data. Subsamples can then be explored in greater detail, as done here. The EDisCS program will provide velocity dispersions and weak lensing maps for ~ 20 LCDCS clusters. Here, with a larger sample, but cruder data, we examine whether the number of luminous galaxies in a cluster, which is correlated with cluster mass (see Kochanek et al. (2002)), correlates with Σ_{cor} .

In Figure 6 we plot the number of galaxies within our images brighter than a limit set above our estimated completeness, N_{GAL} . We do not correct for the differences among estimated luminosity distances for the clusters because such corrections correlate for N_{GAL} and Σ_{cor} , and hence the redshift errors would create an apparent correlation. We exclude the cluster candidate confirmed to be a low surface brightness galaxy (LCDCS 801) and the two suspected as arising from tidal debris among interacting galaxies (LCDCS 857 and 899). Despite the lack of a correction for the redshift effects on either N_{GAL} or Σ_{cor} , the lack of a correction for any foreground/background galaxy contamination (our fields-of-view are too small to do a locally-determined background correction), and the inclusion of the marginal clusters, there is a weak correlation between Σ_{cor} and N_{GAL} (Spearman rank correlation coefficient 0.22, probability of random occurrence 0.15). Although the correlation has significant scatter, of the 14 cluster fields with > 80 galaxies in our images all but one have $\Sigma_{cor} \geq 10.1$, the median Σ_{cor} of our sample. Selecting high Σ_{cor} clusters does not guarantee clusters with many galaxies, but it does nearly guarantee that such clusters will be among the sample. The scatter in the correlation comes primarily from clusters with high Σ_{cor} that upon further examination appear to be poorer clusters than expected. The high measured value of Σ_{cor} is presumably the result of a poorly subtracted galaxy halo, scattered light, coincident Galactic infrared cirrus, or some other contamination. Although it is evident that significant scatter exists and a sample sharply defined by Σ_{cor} will not be sharply defined in any other cluster property (such as richness or mass), it is sufficient for culling, albeit sometimes inefficiently, the richest (and presumably most massive) clusters.

3.3. Comparison With Previous Surveys

3.3.1. Incidence of Lensing

Accepting the two lensing clusters as the only ones in the LCDCS sample at these redshifts, then the incidence of clusters that produce giant arcs over the redshift range $0.5 \leq z \leq 0.7$ that are brighter than $R \sim 21.5$ and have $l/w \geq 10$ is $\geq 0.029 \pm 0.020 \text{ deg}^{-2}$. The uncertainties reflect only Poisson noise (they do not include the effects of large scale structure and do not reflect the various reasons discussed previously that make this a lower limit on the lensing incidence).

Luppino et al. (1999)

The largest directed search for giant arcs in clusters is the study by Luppino et al. (1999) of 38 X-ray selected clusters, $L_X > 2.4 \times 10^{44} h_{50}^{-2} \text{ ergs s}^{-1}$ at $0.15 \leq z \leq 0.823$. They find strong lensing ($l \geq 8''$ and $l/w \geq 10$) in 8 of the 38 clusters (plus some arclets and some suggestive features). Of the most X-ray luminous clusters ($L_X > 1.2 \times 10^{45} h_{50}^{-2} \text{ ergs s}^{-1}$) they find 60% (3 of 5) contain giant arcs, while none (0 of 15) of the least X-ray luminous clusters ($L_X < 1.2 \times 10^{44} h_{50}^{-2} \text{ ergs s}^{-1}$ contain giant arcs.). These are clusters drawn from the *Einstein Observatory* Extended Medium Sensitivity Survey (EMSS; Gioia et al. (1990), Stocke et al. (1991)) which for $\delta > -40^\circ$ covered 734.7 sq. degrees (Henry et al. 1992). Most of their clusters are at $z < 0.5$ because the X-ray survey is most sensitive to the nearer clusters.

They detect 2 clusters with giant arcs at $z > 0.5$. To compare to the LCDCS we need to determine the survey area over which they would have found these clusters. The survey is not complete to all flux limits in the catalog across all fields. For MS0451.6-0305 ($z = 0.55$, $L_X = 23.7 \times 10^{44} h_{50}^{-2} \text{ ergs s}^{-1}$), the effective survey area is 720.6 sq. degrees. For MS2053.7-0449 ($z = 0.583$, $L_X = 6.8 \times 10^{44} h_{50}^{-2} \text{ ergs s}^{-1}$), the effective survey area is 225.4 sq. degrees. Naively, one would simply add $1/720.6$ and $1/225.4$ to obtain the lensing incidence of 0.0058, which is smaller than the LCDCS rate. However, part of the reason that their value is so low is because the EMSS survey is incomplete for clusters at redshifts between 0.5 and 0.7. For a given L_X each cluster is observed over some fraction of the volume between these redshifts. For MS0451 that fraction corresponds to 0.93, while for MS2053 it corresponds to 0.32. Assuming that the number density of lensing clusters is uniform throughout this volume, we can correct the observed values for incompleteness. Doing so, we derive that the lensing incidence measured using the EMSS and the Luppino et al. (1999) study for $z > 0.5$ is $0.014 \pm 0.010 \text{ deg}^{-2}$. We conclude that our measurement is in agreement with that from the EMSS, although both measurements are compromised by small number statistics. Although

we cannot proceed further with this comparison due to the small number of systems involved, the marginally lower lensing incidence in the EMSS area at $z > 0.5$ may in part be connected to the lower number of massive clusters identified in the EMSS relative to the LCDCS at these redshifts (see §3.1).

Gladders, Yee, and Ellingson (2002)

Gladders et al. (2002) present the discovery of one high-redshift (0.77) cluster with strongly-lensed arcs. However, they also provide a preview of what their entire survey might find. This is an interesting, if slightly premature, comparison because their survey is based on an independent method of finding clusters over a comparable survey volume. They have found six clusters with strong lensing to date in their survey, but because Gladders et al. (2002) focus on the one at $z = 0.77$ there are few details of the others (an image of another at $z = 0.62$ is presented by Yee & Gladders (2002)). The six have been found in $\sim 50\%$ of the survey data (the survey in its entirety will cover ~ 100 sq. deg). The photometric redshifts of the lensing clusters are all > 0.5 . Therefore, the complete survey may be expected to yield 12 strong lensing clusters at $z > 0.5$. To best match the situation with the RCS, we include one LCDCS lensing cluster (RX J1347.5) at slightly below $z = 0.5$ because the photometric redshift uncertainty would allow it to be at $z \geq 0.5$ and one LCDCS cluster observed as part of the EDisCS survey (White et al. 2002) that shows arcs even though its arcs may not satisfy the $l/w \geq 10$ criteria that we will use to compare to the simulated lensing incidence. From these four LCDCS lensing clusters we set a lower-limit incidence of lensing at $z > 0.5$ of $0.058 \pm 0.029 \text{ deg}^{-2}$, about half of what is preliminarily the case for the Red Cluster Sequence survey ($0.120 \pm 0.049 \text{ deg}^{-2}$), but within $\sim 1.5\sigma$.

Although the discrepancy is only marginally significant, there are various possible explanations for a difference: (1) the RCS lenses may not satisfy the same criteria (l , l/w , or magnitude limit) as the LCDCS lenses and so the numbers may not be directly comparable, (2) there may be more lenses lurking in the LCDCS (we have not deeply imaged all rich-cluster candidates), and (3) the LCDCS and RCS may select different clusters, with the LCDCS in some way selecting against “good” lensing clusters. We cannot comment further on possibility (1) until the full RCS results are published. Examining Figure 2, and assuming that the correlation between Σ_{cor} and L_X is reasonably tight, we find that we have imaged 13 of 21 candidate clusters expected to have $L_X > 4.7 \times 10^{44} \text{ ergs s}^{-1}$ within $0.5 < z < 0.7$ (this includes low-priority targets). Making a completeness correction suggests that one of the unobserved clusters (assuming that the low-priority targets are indeed clusters) would have an arc. These numbers would suggest that the solution to the possible discrepancy does not lie entirely with unobserved clusters in our sample at $z < 0.7$. However, at $z > 0.7$ we

see that our sample becomes much more seriously incomplete and that because of volume effects the sample potentially includes a large number of very massive clusters. Among our lensing clusters at $z > 0.5$, 1 of 4 is at $z > 0.7$ - if this ratio holds true for the RCS sample, then the full RCS may have only 9 lensing clusters at $0.5 < z < 0.7$ and a lensing rate of $\sim 0.090 \pm 0.030 \text{ deg}^{-2}$, which is less discrepant with our measurement. The agreement in the projected number densities of massive clusters and in the lensing incidence between the X-ray selected EMSS and the LCDCS argues against option (3).

Regardless of any potentially significant difference between the LCDCS and the final RCS lensing rates, there are some key agreements coming from these various studies: (1) massive clusters that produce giant arcs exist out to $z \sim 0.8$, (2) lensing clusters can be identified from optical surveys at these redshifts at the incidence of 1 to 2 per 20 sq. degrees (leading to a prediction of over 2000 such clusters in the entire sky), and (3) the number of lenses found in optically-selected cluster surveys is not qualitatively different than in an X-ray selected cluster survey (although initial X-ray selection will definitely improve the odds of starting with a sample of the likeliest lensing clusters).

Bartelmann et al. (1998)

The potential use of arc statistics as a cosmological constraint led to theoretical efforts to estimate the lensing rate in various cosmologies. Bartelmann et al. (1998) published their predictions for the total numbers of lenses across the sky in three archetypical models (standard CDM (with a tilted power spectrum), open CDM, and Λ CDM). A comparison of the predictions and our results is of interest and provides a glimpse into what may be possible with both more detailed simulations and larger observational samples.

The principal result of the Bartelmann et al. (1998) study is that different cosmologies predict lensing rates that vary by orders of magnitude. In particular, their open CDM model predicts 2400 strongly lensing clusters and their Λ CDM model predicts 280 across the sky. The properties of the simulated arcs (magnitude limit $R < 21.5$ and $l/w \geq 10$) are similar to those presented here (the lenses presented here are brighter than $R = 21.5$ and have $l/w \geq 10$, $l > 8''$). Assuming Poisson statistics and the predicted lensing rates, we calculate that the probability of finding 2 or more strongly lensing clusters within 69 sq. degrees (at any redshift) is 0.08. If we include the other known LCDCS lensing cluster that satisfies the criteria (RX J1347.5; Sahu et al. (1998) identified multiple arcs, with one arc having $l = 7.8''$, $l/w = 15.6$, $V = 21.5$) we find that the probability of finding 3 or more clusters within 69 sq. degrees is 0.012 (the brightest arc in the lensing cluster identified in the EDisCS survey does not satisfy the $l/w \geq 10$ criteria although it has $l = 11''$). Therefore, even the lensing incidence that we have measured, which is a lower limit, is in statistically significant

contradiction to the predictions of a Λ CDM model.

To further strengthen the statistics of the argument, we combine the results from the LCDCS and RCS. From the RCS, the images of two lensing clusters have been published (Gladders et al. (2002), Yee & Gladders (2002)). While quantitative measures of the geometry of the arcs are not presented, they appear to satisfy the $l/w \geq 10$ criteria. However, one system is slightly fainter than $R = 21.5$ and the magnitude for the second system is not published. Including just these two clusters, although Gladders et al. (2002) have identified six lensing clusters in roughly half the survey area (50 sq. degrees), we have a total of five strongly lensing clusters over 119 sq. degrees. The probability of finding this many clusters in such an area of sky in the Λ CDM model is 1.5×10^{-3} . Although including these systems increases the statistical significance of the discrepancy, the discrepancy is significant even with only the three LCDCS systems. It is interesting to note that various surveys are leading to the same conclusion and that in combination they may already provide exceedingly strong statistical constraints.

We conclude that the observations are discrepant with the predictions of the Λ CDM model as constructed by Bartelmann et al. (1998). We note that the application of the Bartelmann et al. (1998) results is not entirely consistent with this observational sample because they focused on clusters at $z \sim 0.3$ and source galaxies at $z < 1$. We are likely to have some source galaxies at $z > 1$, although the primary lensed images are quite bright ($R \leq 21.5$) and so are unlikely to be very distant objects (a counterexample is presented by Gladders et al. (2002) in that one of their arcs is a galaxy at $z = 4.8786$). As argued by Bartelmann et al., galaxies that produce arcs with $R < 21.5$ are likely to be galaxies with intrinsic $R < 23$, which are in turn likely to be at $z < 1$. Evidently, the models must be constructed to more accurately represent these samples, but our results and conclusions are in direct agreement with those of Bartelmann et al.’s based on the results from the independent EMSS.

To increase the lensing rates in the models (see Bartelmann et al. (1998)), there have been appeals to certain cluster properties such as strong asymmetry and presence of a massive central concentration (such as the BCG). In support of some missing ingredient in the models, we note that there are now at least two known strongly lensing clusters at $z > 0.7$, where all of the Bartelmann et al. (1998) models predict a negligible likelihood of lensing. However, subsequent studies (Meneghetti et al. (2000), Flores et al. (2000)) that examined the effect of substructure and asymmetries found only moderate changes from the previous results. In contrast to another challenge to the CDM framework, the compactness of galaxy cores, any solutions to that challenge that affects the concentration of all CDM cluster halos will exacerbate the discrepancy between the predicted and observed number of strong lenses

(Bartelmann 2002a). A recent study (Bartelmann et al. 2002b) finds promise in progressing beyond the simple cosmological constant and altering the equation of state.

The simulations are currently challenged to achieve both sufficient resolution to trace cluster substructure and model a sufficiently large volume of the Universe to include enough of the most massive clusters (for example see Hamana et al. (2002)). In particular, the scatter in halo properties must be accounted for because the most concentrated systems will dominate the lensing incidence (Wyithe et al. 2001). When such simulations exist, one should match not only the total number of lensing clusters, but also their redshift distribution in order to constrain the growth of structures in the Universe and the underlying cosmological framework. We conclude that the data are now at a sufficient stage to motivate a new exploration of the theoretical models.

4. Summary

We have examined a subsample of cluster candidates drawn from the Las Campanas Distant Cluster Survey (LCDCS) for evidence of strong gravitational lensing. We conclude the following:

- 1) Over the redshifts range we have explored most extensively ($0.5 < z < 0.7$) we have identified two previously unknown strongly lensing systems and a third possible system (see Table 1) among a subsample of LCDCS clusters. Using only the two secure lensing systems from these three, we set a lower limit on the incidence of strong lensing in this redshift range of $0.029 \pm 0.020 \text{ deg}^{-2}$.
- 2) Over the entire redshift range of the LCDCS ($0.35 < z \leq 0.85$) we now know of four secure lensing systems (including one previously known one, RX J1347.5 and one that is part of the EDisCS sample (White et al. 2002)). Of these four, the arcs in EDisCS lensing cluster may not satisfy the generally adopted magnitude and size criteria. Retaining only the three other lensing systems, we set a lower limit on the incidence of strong lensing in this redshift range of $0.043 \pm 0.025 \text{ deg}^{-2}$.
- 3) Our lower limit on the lensing incidence at $z > 0.5$ agrees within the uncertainties with the measurement based on the results from a study of EMSS clusters ($0.014 \pm 0.010 \text{ deg}^{-2}$; Luppino et al. (1999)) and the preliminary results from the Red Cluster Sequence survey (somewhere between 0.06 to 0.12 deg^{-2} ; Yee & Gladders (2002)).
- 4) The empirical values for the number of strongly lensing clusters are significantly higher than the prediction of the Λ CDM model from Bartelmann et al. (1998). The probability

of finding 3 or more strongly lensing clusters in the LCDCS's 69 sq. degrees is 0.012. The discrepancy between the observed and predicted rates for the Λ CDM model is in agreement with the conclusion of Bartelmann et al. (1998) based on their comparison to the results from the EMSS clusters. Although our study has confirmed the discrepancy between observations and theoretical expectations in the “concordance” model, we have used the same theoretical results, namely those presented by Bartelmann et al. (1998). This discrepancy indicates a problem with the theoretical models either with the generally accepted concordance cosmological model (because the predictions from an open CDM model are in much better agreement with the observations), the specifics of the cluster formation and resulting gravitational potential, or the assumed background population. The next step is to reexamine the models to see if an order of magnitude increase in the lensing rate for what has become the standard cosmological model, $\Omega_m = 0.3, \Omega_\Lambda = 0.7$, is at all possible.

5. Acknowledgments

The authors thank Chuck Keeton for comments on a preliminary manuscript. DZ acknowledges financial support from National Science Foundation CAREER grant AST-9733111 and a fellowship from the David and Lucile Packard Foundation.

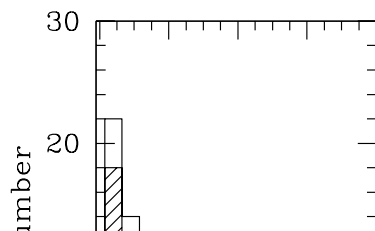
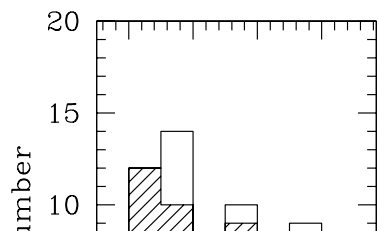
REFERENCES

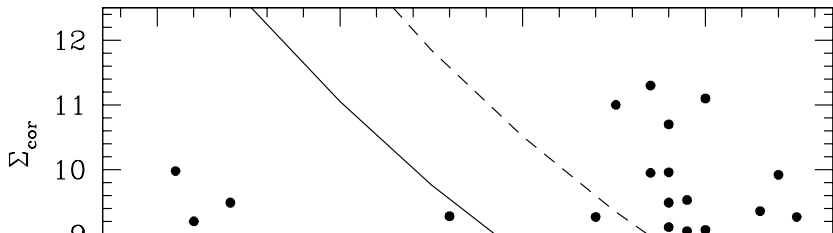
- Bartelmann, M., Huss, A., Colberg, J.M., Jenkins, A., & Pearce, F.R. 1998, *A&A*, 330, 1
- Bartelmann, M., 2002, in “Dark Matter and Energy in Clusters of Galaxies” in press ([astro-ph/0207032](#))
- Bartelmann, M., Meneghetti, M., Perrotta, F., Baccigalupi, C., & Moscardini, L., 2002, *â*, submitted ([astro-ph/0210066](#))
- Bertin, E., & Arnouts, S. 1996, *A&AS*, 313, 21
- Borgani, S., Rosati, P., Tozzi, P., & Norman, C. 1998, *ApJ*, 517, 40
- Clowe, D., Luppino, G.A., Kaiser, N., and Gioia, I.M. 2000, *ApJ*, 539, 540
- Dahle, H., Kaiser, N., Irgens, R.J., Lilje, P.B., & Maddox, S.J. 2002, *ApJS*, 139, 313
- de Bernardis, P., et al. 2000, *Nature*, 404, 955

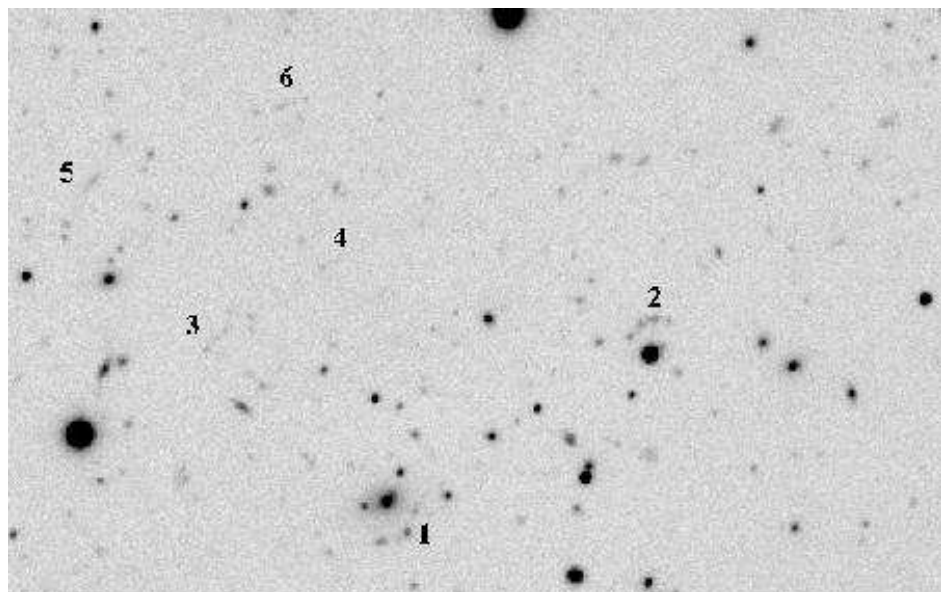
- Ebeling, H., Edge, A.C., Bohringer, H., Allen, S.W., Crawford, C.S., Fabian, A.C., Voges, W., and Huchra, J.P. 1998, MNRAS, 301, 881
- Eke, V. R., Cole, S., & Frenk, C. S. 1996, MNRAS, 282, 263
- Ettori, S., Allen, S.W., & Fabian, A.C. 2001, MNRAS, 322, 187
- Evrard, A.E., et al. 2002, ApJ, 573, 7
- Falco, E.E., Kochanek, C.S., & Muñoz, J.A. 1998, ApJ, 494, 47
- Flores, R.A., Maller, A.H., & Primack, J.R. 2000, ApJ, 535, 555
- Frenk, C.S., White, S.D.M., Esftathiou, G., and Davis, M. 1990, ApJ, 351, 10
- Gladders, M.D., & Yee, H.K.C. 2000, AJ, 120, 2148
- Gladders, M.D., Yee, H.K.C., & Ellingson, E. 2002, AJ, 123, 1
- Gioia, I.M., Maccacaro, T., Schild, R.E., et. al. 1990, ApJS, 72, 567
- Gonzalez, A.H., Ph.D. Dissertation, University of California at Santa Cruz
- Gonzalez, A.H., Zaritsky, D., Dalcanton, J.J., & Nelson, A.E. 2001, ApJS, 137, 117
- Gonzalez, A.H., Zaritsky, D., Simard, L., Clowe, D., & White, S.D.M. 2002, ApJ, in press
- Gonzalez, A.H., Zaritsky, D., Wechsler, R.H. 2002, ApJ, 571, 129
- Hamana, T., Yoshida, N. , & Suto, Yasushi 2002, ApJ, 568, 455
- Hanany, S., et al. 2000, ApJ, 545, L5
- Henry, J. P., Gioia, I. M., Maccacaro, T., Morris, S. L., Stocke, J. T., & Wolter, A. 1992, ApJ, 386, 408
- Hoekstra, H., Franx, M., & Kuijken, K 2000, ApJ, 432, 88
- Jeltema, T.E., Canizares, C.R., Bautz, M.W., Malm, M.R., Donahue, M., & Garmire, G.P. 2001, ApJ, 562, 124
- Joy, M., LaRoque, S., Grego, L., Carlstrom, J.E., Dawson, K., Ebeling, H., Holzappel, W.L., Nagai, D., and Reese, E.D. 2001, ApJ, 551, L1
- Keeton, C.R. 2001, ApJ, 562, 160

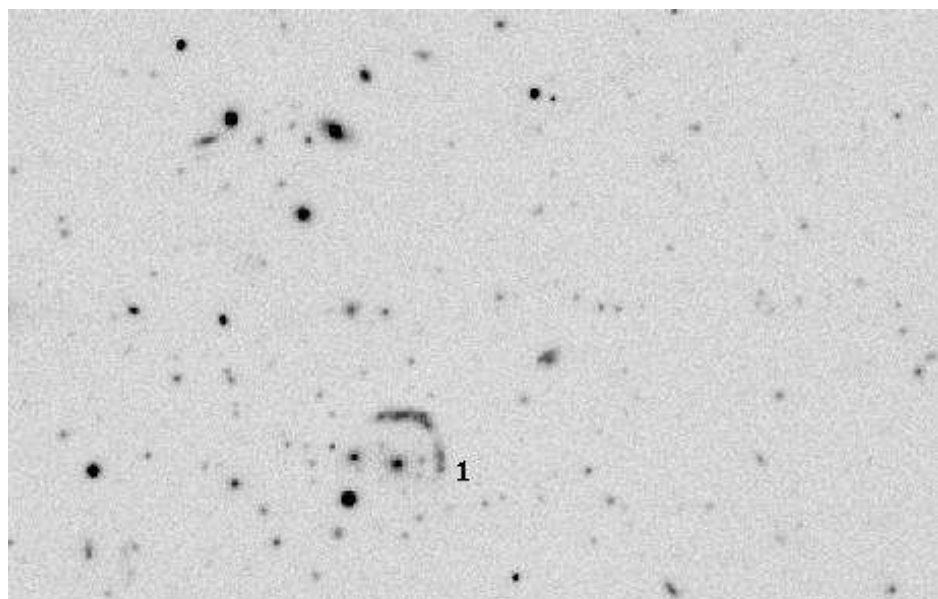
- Kitayama, T. & Suto, Y. 1996, *ApJ*, 469, 480
- Kochanek, C.S., White, M., Huchra, J., Macri, L., Jarrett, T.H., Schneider, S.E., & Mader, J., astro-ph/0208168
- Landolt, A.U. 1992, *AJ*, 104, 340
- Lewis, A.D., Stocke, J.T., Ellingson, E., & Gaidos, E.J. 2002, *ApJ*, 566, 744
- Lubin, L.M., Oke, J.B., & Postman, M. 2002, *AJ*, in press (astro-ph/0206442)
- Luppino, G. A. & Gioia, I. M. 1995, *ApJ*, 445, 70
- Luppino, G.A., Gioia, I.M., Hammer, F., Le Fèvre, O., & Annis, J.A. 1999, *A&AS*, 136, 629
- Lynds, R.S. & Petrosian, V. 1986, *Bull. Am. Astr. Soc.*, 18, 1014
- Meneghetti, M., Bolzonella, M., Bartelmann, M., Moscardini, L., & Tormen, G. 2001, *MNRAS*, 314, 338
- Meneghetti, M., Yoshida, N., Bartelmann, M., Moscardini, L., & Springel, V., Tormen, G., & White, S.D.M. 2001, *MNRAS*, 325, 435
- Nelson, A.E., Gonzalez, A.H., Zaritsky, D., & Dalcanton, J.J. 2001, *ApJ*, 563, 629
- Nelson, A.E., Gonzalez, A.H., Zaritsky, D., & Dalcanton, J.J. 2001, *ApJ*, 566, 103
- Ostriker, J.P., & Steinhardt, P.J. 1995, *Nature*, 377, 600
- Perlmutter, S. et al. 1999, *ApJ*, 517, 565
- Postman, M., et al. 1996, *AJ*, 111, 615
- Press, W. H. & Schechter, P. 1974, *ApJ*, 187, 425
- Pryke, C., et al. 2002, *ApJ*, 568, 46
- Riess, A.G., et al. 1998, *AJ*, 116, 1009
- Scodeggio, M., et al. 1999, *A&AS*, 137, 83
- Sahu, K.C., et al. 1998, *ApJ*, 429, L125
- Schindler, S., Hattori, M., Neumann, D.M., & Böhringer, H. 1997, *A&A*, 317, 646
- Smith, J. A., et al. 2002, *AJ*, 123, 2121

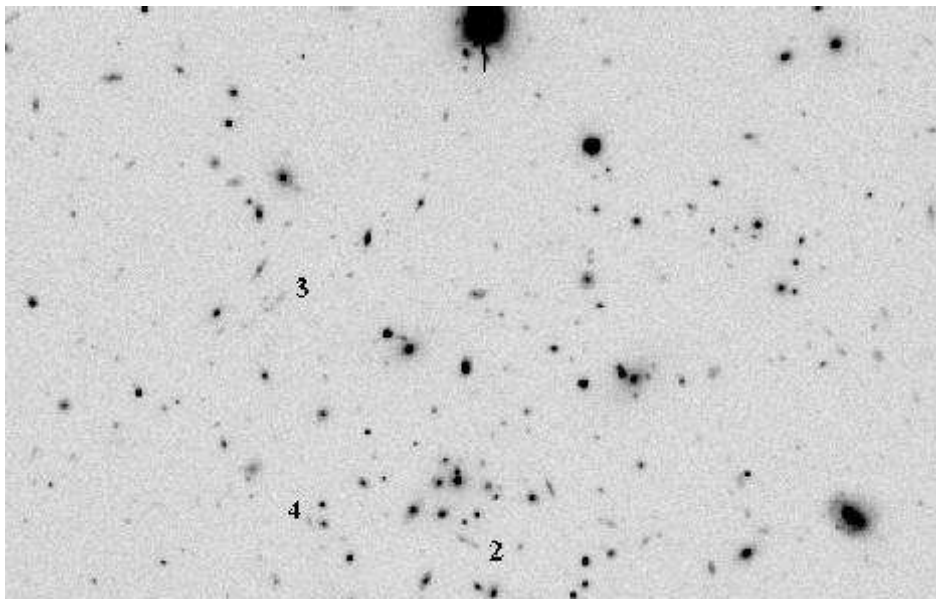
- Soucail, G., Fort, B., Mellier, Y., Picat, J.P. 1987, *A&A*, 172, L14
- Stocke, J.T., Morris, S.L., Gioia, I.M., et al. 1991, *ApJS*, 76, 813–330, 1
- White, S.D.M., et al. 2002, in prep.
- Willick, J.A., Thompson, K.L., Mathiesen, B.F., Perlmutter, S., Knop, R.A., and Hill, G.J. 2001, *PASP*, 113, 658
- Wyithe, J.S.B., Turner, E.L., & Spergel, D.N. 2001, *ApJ*, 555, 504
- Xue, Y. & Wu, X. 2000, *ApJ*, 538, 65
- Yee, H.K.C., & Gladders, M. 2002 in *AMiBA 2001: High-z Clusters, Missing Baryons, and CMB Polarization* (ASP: L.-W. Chen, C.-P. Ma, K.-W. Ng, and U.-L. Pen, eds), in press
- Zaritsky, D., Nelson, A. E., Dalcanton, J. J., & Gonzalez, A. H. 1997, *ApJ*, 480, 91











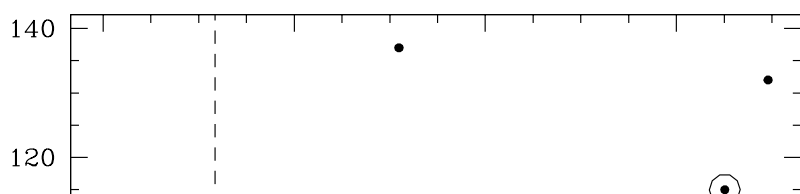


Table 1. Cluster Observations

LCDCS Number	α (2000.0)	δ (2000.0)	Exp. (sec.)	Seeing (")	z_{est}	Σ_{cor} (10^{-3} cts/s/sq. ")	N_{GAL}	Comments
0005	10:02:27.1	-12:47:13	2400	0.53	0.57	9.17	75	
0017	10:05:43.6	-11:47:43	1800	0.75	0.53	10.10	68	
0027	10:07:54.7	-12:21:19	2400	0.60	0.52	10.50	93	
0091	10:31:50.3	-12:44:27	2400	0.50	0.69	10.10	98	
0104	10:36:10.4	-12:44:43	1800	0.66	0.55	9.03	55	
0111	10:38:00.0	-12:18:54	1800	0.65	0.66	9.45	74	
0163	10:51:22.7	-12:01:27	2400	0.65	0.67	12.30	137	
0240	11:17:22.0	-11:55:46	1800	0.70	0.79	10.90	86	Marginal
0248	11:18:36.2	-12:02:03	1800	0.51	0.60	10.20	50	Marginal
0280	11:23:59.4	-11:50:07	3200	0.67	0.54	10.10	83	Lens System
0374	11:48:06.0	-11:45:33	2400	0.62	0.53	9.38	70	
0415	11:57:34.7	-12:18:48	2400	0.62	0.60	10.70	73	
0417	11:57:54.3	-11:51:22	1800	0.65	0.82	11.60	44	Marginal
0418	11:58:14.6	-12:14:11	1800	0.66	0.65	10.30	72	
0468	12:10:12.7	-12:19:07	1800	0.68	0.74	9.42	73	Marginal
0486	12:12:29.9	-12:16:19	2400	0.62	0.61	11.10	92	Lens System
0550	12:35:27.7	-12:57:01	2400	0.47	0.57	9.12	111	
0586	12:44:51.7	-12:56:56	1800	0.64	0.58	9.36	69	
0589	12:45:02.0	-11:49:19	2400	0.51	0.50	10.50	70	
0616	12:55:31.5	-12:16:55	1800	0.64	0.54	11.00	57	Marginal
0635	13:01:44.9	-12:13:24	1800	0.64	0.50	9.86	76	Marginal
0684	13:15:47.5	-11:37:26	2400	0.53	0.53	10.50	87	
0698	13:19:50.3	-12:06:35	2400	0.65	0.55	18.1	132	
0717	13:22:56.9	-11:44:43	2400	0.52	0.72	9.50	74	
0719	13:23:50.2	-12:52:51	1800	0.48	0.59	9.17	68	
0778	13:35:50.4	-11:46:16	1800	0.84	0.58	10.40	69	
0785	13:37:08.7	-12:57:14	1800	0.46	0.62	14.10	51	
0795	13:39:22.1	-13:00:14	2400	0.51	0.59	11.30	55	

Table 1. Cluster Observations (continued)

LCDCS Number	α (2000.0)	δ (2000.0)	Exp. (sec.)	Seeing ($''$)	z_{est}	Σ_{cor} (10^{-3} cts/s/sq $''$)	N_{GAL}	Comments
0801	13:40:09.6	−12:10:09	1800	0.63	0.67	13.20		LSB
0814	13:42:12.8	−12:59:28	1800	0.46	0.54	9.35	69	
0827	13:46:42.4	−11:59:24	2400	0.47	0.71	11.30	81	
0836	13:48:52.0	−12:04:18	1800	0.43	0.59	12.80	53	
0857	13:54:50.9	−12:09:11	1800	0.45	0.72	9.55		Tidal Pair
0879	14:01:30.8	−11:44:46	2400	0.44	0.57	9.72	45	
0883	14:03:15.8	−12:14:18	1800	0.64	0.65	10.10	89	
0899	14:05:37.0	−12:23:38	1800	0.62	0.79	9.22		Tidal Pair
0923	14:10:35.6	−12:25:05	2400	0.50	0.69	10.20	70	
0944	14:16:30.6	−12:35:59	1200	0.62	0.62	10.00	62	Marginal
0954	14:20:29.7	−11:34:04	2400	0.39	0.67	17.30	115	Lens System
0961	14:24:16.7	−12:09:51	1800	0.49	0.74	11.10	74	
0974	14:28:59.7	−12:27:07	2400	0.52	0.63	10.90	85	
1007	14:46:08.4	−12:32:08	2400	0.46	0.53	13.10	94	
1038	14:59:03.0	−12:51:08	1800	0.53	0.63	9.71	58	
1050	15:01:43.4	−11:51:54	2400	0.51	0.68	9.34	34	Marginal

Table 2. Candidate Arc Photometry

LCDCS Cluster	Lens Designation	g'	r'	$g' - r'$	R
280	1	23.07	21.83	1.24	21.50
280	2	22.42	22.24	0.18	22.06
280	3	24.31	23.95	0.36	23.76
280	4	24.76	24.25	0.51	24.04
280	5	23.97	23.95	0.02	23.78
280	6	24.63	24.13	0.50	23.92
486	1	20.74	20.07	0.67	19.81
486	1a	21.13	20.43	0.70	20.18
486	1b	22.08	21.40	0.68	21.14
954	1	23.36	21.67	1.69	21.33
954	2	23.94	23.44	0.50	23.22
954	3	23.98	23.42	0.56	23.19
954	4	23.98	24.05	-0.07	23.91